PCCP

Accepted Manuscript

ROYAL SOCIETY OF CHEMISTRY

www.rsc.org/pccp

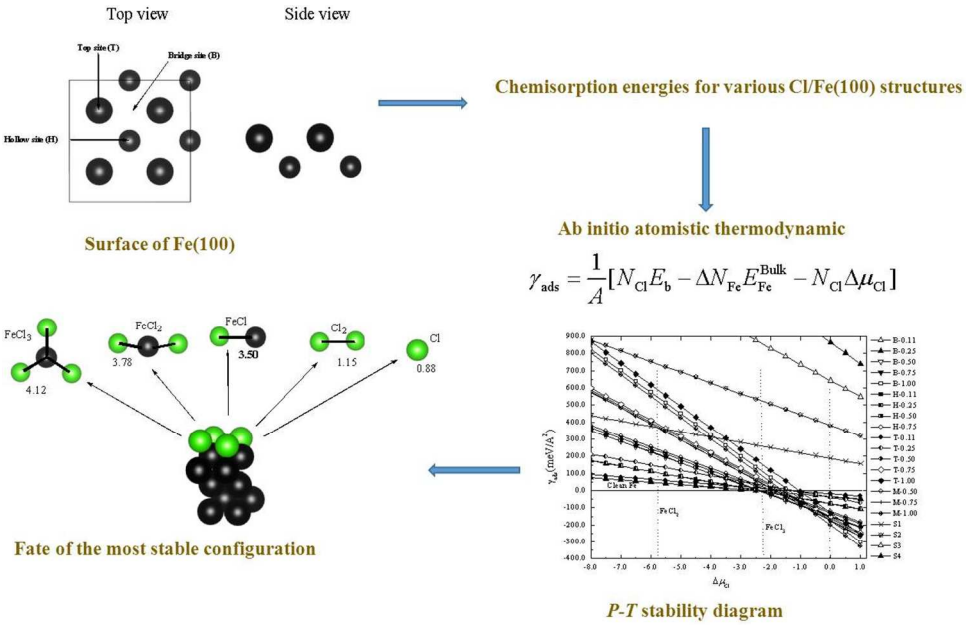

Results will help to understand and reduce emission of iron chlorides from the use of commercial oil lubricants

Table of Content Entry
221x165mm (150 x 150 DPI)

Theoretical Insight into Chlorine Adsorption on the Fe(100) Surface

Mohammednoor Altarawneh,[1,2*] Sherin A. Saraireh[3]

[1]School of Engineering and Information Technology, Murdoch University, Murdoch, WA 6150, Australia

[2]Chemical Engineering department, Faculty of Engineering, Al-Hussein bin Talal University, Ma'an, Jordan.

[3]Physics department, Faculty of Sciences, Al-Hussein bin Talal University, Ma'an, Jordan.

* Corresponding author: Phone: (+61) 2 4985-4286

Email: m.altarawneh@murdoch.edu.au

Abstract

This study represents a detailed DFT periodic-slab study on the interaction between atomic chlorine and the Fe(100) surface. Energetic and structural parameters are calculated for wide ranges of coverages corresponding to top, bridge and hollow pure on-surface adsorptions. Calculated chemisorbed energies are found to increase gradually with the degree of coverage. Formation of iron chlorides via substituational adsorption is predicted to be not feasible in view of calculated chemisorptions energies. This finding is in line with earlier experimental measurements with regard to the absence of chlorine diffusion into bulk Fe. Sublimation energies for $FeCl_2$ and $FeCl_3$ are estimated and discussed to elucidate fate for chlorine-iron thin layer. A stability temperature-pressure diagram is constructed for a wide range of chlorine chemical potentials to mimic real operational conditions.

Introduction

Due to its high reactivity, surface chemistry of metallic iron has been a subject of great deal of research in terms of its catalytic, oxidative and corrosive properties. Understanding of gaseous-solid interactions on iron surfaces is of prominent industrial and environmental applications as evident in metallurgical processes[1] and removal of organic pollutants.[2] Chemisorptions of various species on iron surfaces were thoroughly investigated. Common examples include O_2,[3] H_2O,[4] and CO.[5] In particular, interest in adsorption of chlorine on iron surfaces stems from the fact that chlorinated hydrocarbons are often employed as additives to lubricants. As a model of these chlorinated hydrocarbons, it has been demonstrated that carbon tetrachloride (CCl_4) adsorbs dissociatively on iron surfaces to form a thin film of chlorine overlayers together with CCl_2 fragments and unidentified forms of iron chlorides.[6]

While the adsorption of chlorine on the low-index copper surfaces was investigated in details,[7-9] there have been a few studies on the chemisorptions of chlorine on iron surfaces. The pioneering work by Dowben and Jones[10] found that interaction of chlorine with Fe(100) ceased upon the formation of a chemisorbed layer that corresponds to a $c(2 \times 4)$ pattern. They concluded that chlorine atoms do not diffuse into bulk iron to form iron chlorides. In contrast, Hino and Lambert,[11] found that low-pressure interactions of chlorine with Fe(100) continue to form $FeCl_2$ bulk. Their thermochemical analysis indicated a preferential desorption of $FeCl_2$ rather than FeCl and Cl. The behaviour of iron and chlorine system was observed to be in line with the behaviour of many bcc transition metals toward chlorine. A recent theoretical study by Pick[12] studied the co-adsorption of chlorine and oxygen on the ferromagnetic Fe(100) surface. Adsorption energies were calculated for low ($\Theta = 0.25$) and high ($\Theta = 1.00$) coverages of chlorine adatoms on hollow sites. A significant discrepancy in the adsorption properties between O and Cl adsorbates was rationalised in view of the difference in their electronic properties. Similar observations were also obtained for the co-adsorption of H_2O and Cl on the Fe(100) surface.[13]

A micro-scale description of chlorine adsorption on iron surfaces necessitates considering real operational conditions of various temperatures and pressures. Experimentally, this could be achieved by carrying out accurate *in situ* measurements under

temperatures and pressures of interest. Alternatively, the approach of ab initio atomistic thermodynamics[14] provides a tool to extrapolate the results from theoretical calculations, typically obtained at 0.0 K and 1.0 atm, to real *T* and *P* conditions.

In this study, we present a comprehensive density functional theory (DFT) periodic slab model investigation into the behaviour of chlorine chemisorption on a clean Fe(100) surface. A number of structural, energetic and structural properties are estimated for on-surface and sub-surface substituational adsorption over a wide range of chlorine coverages. Stability thermodynamic phase diagram is established for all plausible chlorine-Fe(100) configurations. Results herein will be instrumental to understand the behaviour of chlorine adsorption on iron surfaces. For instance, calculated values will enable to elaborate on the experimental finding that the maximum possible coverage for chlorine on the Fe(100) surface was found to amount to 0.74.[10]

Computational Details

Total energies and structural optimisations were carried out using Vienna ab initio simulation package (VASP).[15] Spin polarised PAW-GGA[16] is used for all calculations. It has been shown that the use of PAW-GGA is essential to satiosfactorily desribe the ferromagnaetic nature of Fe.[17] 5-layers slab is used in the calculations in which the three top-most layers where allowed to relax while fixing the bottom two layers at their bulk positions. Test on one structure (B-0.25) using a seven-layers slab while allowing the five top most layers to relax change the binding energy of this structure by only 48.2 meV (1.21 %). Calculations are carried out deploying an energy cut of 400 eV and auomatic generation of **k**-points using a monkhorst-pack of 4 × 4 × 1. Test on one structure (B-0.25) with an energy cut off at 600 eV and 6 × 6 × 1automatic generation of **k**-points changes its total energy by only 1.3 meV and its binding energy by 14.6 meV (0.37%). A vaccum spacing between unit cells is set to 14.0 Å along *z*-direction. A unit cell of (2 × 2) is used for all calculations, but for a chlorine covergae 1/9 in which a unit cell of (3 × 3) is used. Dipole corections were applied along the *z*-direction. Calculations of Fe, $FeCl_2$ and $FeCl_3$ unit cells are carried out with an energy cut of 600 eV and an auomatic monkhorst-pack egneration of **k**-points using a scheme of 12 × 12 × 12 centered at the Γ point. Calculations of heat of formations (E^f) for bulk iron

chlorides incorporate energies for bulk iron chlorides, single Fe atoms ($E_{\mathrm{Fe}}^{\mathrm{Bulk}}$) and single chlorine molecules (E_{Cl_2}):

$$E^{\mathrm{f}} = E_{\mathrm{FeCl}n}^{\mathrm{Bulk}} - E_{\mathrm{Fe}}^{\mathrm{Bulk}} - \frac{n}{2}E_{\mathrm{Cl}_2}$$

Cohesive energy (E_{coh}) is calculated according to:

$$E_{\mathrm{Coh}} = E_{\mathrm{Fe}}^{\mathrm{Bulk}} - E_{\mathrm{Fe}}^{\mathrm{gas}}$$

where $E_{\mathrm{Fe}}^{\mathrm{Bulk}}$ and $E_{\mathrm{Fe}}^{\mathrm{gas}}$ denote total energies for bulk Fe (per unit formula) and a gas phase Fe atom; respectively.

The average binding (E_{b}) and chemisorption (E_{chem}) energies are calculated according to:

$$E_{\mathrm{b}} = \frac{1}{n}[E_{\mathrm{Cl}}/_{\mathrm{Slab}} - (E_{\mathrm{slab}} + nE_{\mathrm{Cl}})] \qquad E_{\mathrm{chem}} = \frac{1}{n}[E_{\mathrm{Cl}}/_{\mathrm{Slab}} - (E_{\mathrm{slab}} + \frac{n}{2}E_{\mathrm{Cl}_2})]$$

where n is the number of adsorbed chlorine atoms and $E_{\mathrm{Cl}}/_{\mathrm{Slab}}$, E_{slab}, and E_{Cl} signify total energies for Cl/Fe(100) system, the clean Fe(100) surface, an isolated single chlorine atom and an isolated chlorine molecule; respectively. E_{b} and E_{chem} energies for substitutional adsorption systems are calculated analogouslly taking into account the enrgies and numbers of substituted bulk Fe atoms:

$$E_{\mathrm{b}}^{subst} = \frac{1}{n}[E_{\mathrm{Cl}}/_{\mathrm{Slab}} + nE_{\mathrm{Fe}}^{\mathrm{Bulk}} - (E_{\mathrm{slab}} + nE_{\mathrm{Cl}})] \qquad E_{\mathrm{chem}}^{subst} = \frac{1}{n}[E_{\mathrm{Cl}}/_{\mathrm{Slab}} + nE_{\mathrm{Fe}}^{\mathrm{Bulk}} - (E_{\mathrm{slab}} + \frac{n}{2}E_{\mathrm{Cl}_2})]$$

To establish a relation between values of E_{b} and the effect of varying temperature and partial pressure of chlorine, the apparoch of ab initio atomistic thermodynamics is applied to generate a stability *T*-*P* phase diagram for all possible configurations. Detailed descriptions of this methodology are given in many recent studies.[14,18] In the final governing equation, the surface Gibbs free energies of adsorption (γ_{ads}) are estimated as:

$$\gamma_{\mathrm{ads}} = \frac{1}{A}[N_{\mathrm{Cl}}E_{\mathrm{b}} - \Delta N_{\mathrm{Fe}}E_{\mathrm{Fe}}^{\mathrm{Bulk}} - N_{\mathrm{Cl}}\Delta\mu_{\mathrm{Cl}}]$$

where ΔN_{Fe} is the difference in the number of Fe atoms between the Cl/Fe(100) system and the clean Fe(100) surface (i.e, as in substitutional adsorption) and $\Delta\mu_{Cl}$ is the chlorine chemical potential. $\Delta\mu_{Cl}$ is the term that characterises the dependence of γ_{ads} on temperature and pressure.

Results and Discussion

Fe bulk and Fe(100) surface

Calculated lattice constant, bulk modulus, Magnetic moment and cohesive energy for bulk bcc iron are given in Table 1 along with other literature values.[19-22] Calculated values for lattice constant, cohesive energy and magnetic moment compare very well with correponding experimental measurments. Our value of bulk modulus is estimated from fitting of energy versus volume according to the Brich-Murnaghan equation of state. Clealy, our calculated bulk modulus (192 GPa) is within the significantly scatted publsihed theoretical values; i.e, 144 to 215 GPa.[21] Zhang et al.[21] attributed this observation to a volume-induced magnetic transition occuring at an elongation of about 2% lattice constant. Estimated relaxations and magnetic moments for the first layers of the Fe(100) surfrace are given in Table 2 with a comparsion with other avilable literature values.[23-25] As given in Tables 1 and 2, our calculated properties for bulk Fe and Fe(100) surface are in good agreement with other theoretical and experimental values.

Energies and structural parameters for on-surface and substituational adsorptions

The Fe(100) surface contains three distinct on-surface adsorption sites; namely top (T), bridge (B) and hollow (H). These sites are shown in Figure 1.We consider Cl/Fe(100) configurations at coverages varying from 1/9 to 1 ML for the three adsorption modes. Additionally, we consider mixed combinations (M) of B and H sites for coverages of 0.5, 0.75 and 1 ML. E_b and E_{chem} energies are given in Table 3 for the seventeen different Cl/Fe(100) configurations. For a very low coverage, i.e.; $\Theta \leq 0.25$, adsorption at B and H sites are the most prefered metastates with very comparable E_b and E_{chem} values. This is consistent with the work of Pick [12], who found that the adsorption of chlorine on a hollow site at a coverage of 0.25 ML is more prefered than the lower coverage of 0.1 ML. Pure H and B

adsorption modes are more prefered than adsorption at M and T positions at all coverages. Overall, a stability ordering of (B, H) > M > T is deduced based on values in Table 3. It should be noted that due to the repulsion forces between negatively charged chlorine atoms, not all chlorine atoms are adsorbed in their optimal H or B sites at $\Theta \geq 0.5$ ML . An analogous behaviour was also observed previously for the system of Cl/Cu(111).[7]

A summary of most prominent geometrical features for all on-surface Cl/Fe(100) configurations is given in Table 4. The average Cl-Fe nearest distances (d(Cl-Fe)) increase in the order T > M > B > H modes. The average height of Cl atoms above the first Fe layer (Z) decreases gradually as the degree of chlorination increases. As shown in Table 4, relaxation between the first and second Fe layers (d_{12}(%)) significantly enlarges at a full coverage. As witnessed by h values, vertical buckling in all configurations is very minimal, i.e.; in the range of 0.232 Å – 0.005 Å. The calculated minimum distance between adsorbed chlorine atoms is found to amount to 3.500 Å. This distance is close to the corresponding experimental value of 3.320 Å.

In addition to pure on-surface adsorption, we also consider substituational adsorption modes that signify coverages of 0.25 ML, 0.50 ML, 0.75 ML, 1.00 ML and 2.00 ML. These coverages correspond to configurations of S1/S6, S2, S3, S4 and S5 respectively. Figure 2 depicts structures for S1-S6 substituational configurations. In structures S1-S4 and S6, chlorine atoms substitute first and second Fe atoms layers; respectively. In structure S5, all Fe atoms in the first and third layers are replaced with Cl atoms. The first three layers of S5 configuration resemble an $FeCl_2$ surface along the low-index orientation of (100). The surface chlorine atom shown in structure 6 (Figure 2), was initially positioned in the second layer as a subsurface adsorption. However, the final equilibrium configuration resulted in a vacant Fe site in the second layer and the surface adsorption of the substituted chlorine atom as shown in the side view of S6. Table 5 gives E_{chem} energies and descriptions for substitutional configurations. According to E_{chem} trend in Table 5, the thermodynamic prefarability toward substitutational adsoroptions remarkably decreses with the number of substituted Fe atoms. As dedcuced from E_{chem} values for S1 and S6, subsurface substitution is less preferred than on-surface substitution, i.e.; -2.16 eV versus -1.33 eV.

Figure 3 plots E_{chem} versus Θ for on-surface (B, H, T and M) and substituational (S) adsorption modes The striking feature in this Figure is that values of E_{chem} for on-surface adsorptions are roughly independent of the coverage for Θ ≤ 0.5 ML. According to energy trends in Figure 3, the highest possible prefered coverage is 0.5 ML. After this coverage, the magnitute of E_{chem} decreses gradually, however, the adsorption process is still exothermic even at a coverage of 1 ML. Our estimation for the height possible coverage, i.e; 0.50 ML, is lower than the correponding experimental finding of ~ 0.75 ML. The broad conculsion from Figure 5 is that the formation of iron chlorides, i.e.; as in the S5 streucture, via Fe susbtitution is significantlly less thermodynamically prefered than pure on-surface Cl adsorptions. This observation is consistent with the early experimentally work of Dowben and Jones [10] with regard to the absence of chlorine diffusion into bulk Fe.

The fate of Chlorine-Iron thin layer

Desorption of species from chlorinated Fe(100) surface was a subject of experimental investigation. Hino and Lambert[11] exaplained that heating of chemisorbed Cl/Fe(100) overlayer results in the concurrent evaporation of $FeCl_2$ dimers rather than FeCl or Cl atoms. By deplying a thermodynamic cycle that incorporates atomisation and sublimation energies of relevant species, they showed that $FeCl_2$ desorption is strongly prefered over chlorine molecule desorption. They concluded that the behaviour of iron toward chlorine is consistent with the behaviour of other transition metals. The early experimental work by Dowben and Jones [10] suggested that chlorine adsorption on Fe(100) surface occurs without the formation of any iron chlorides. To get an insight into the fate of chemisorbed Cl/Fe(100) layer, we calculate in Figure 4 sublimation energies for the emission of $FeCl_3$, $FeCl_2$ and FeCl. In calculations of sublimation energies for ferric chlorides ($E^{\text{Sublimation}}_{\text{FeCl}n}$), the chemisorbed Cl/Fe(100) layer is assumed to be the structure M-1.00. It follows that sublimation energies for ferric chlorides are calculated as:

$$E^{\text{Sublimation}}_{\text{FeCl}n} = E^{\text{gas}}_{\text{FeCl}n} + E_{\text{-FeCl}n} - E_{\text{M–1.00}}$$

where $E^{\text{gas}}_{\text{FeCl}n}$, $E_{\text{M–1.00}}$ and $E_{\text{-FeCl}n}$ refer to total energies for a gaseous $FeCl_n$ molecule, the M-1.00 configuration and the structure that forms upon the desorption of an FeCl*n* molecule

from the M-1.00 configuration; respectively. Evaporation energies for Cl and Cl_2 is calculated analogously."

As shown in Figure 4, desorption of Cl and Cl_2 is predicted to incur significantly less thermodynamic penality than evaporation energies pretinent to sublimation of $FeCl_3$ (4.12 eV), $FeCl_2$ (3.78 eV) and FeCl (3.50 eV). Our calculated value for the desorption energy of $FeCl_2$ is in a relatively good agreement with the experimental sublimation energy of a pure $FeCl_2$, i.e.; 5.11 eV.[26] Calculated values in Figure 6 supports partially the expeimental findings of Dowben and Jones[10] with regard to the preferential desorption of chlorine and the absence of of iron chlorides formation. Chlorine atoms desorption was also found be the sole decomposition channel in Cl/Cu(111) system.[7]

To explain the discrepancy with the work of Hino and Lambert[11] in reference to the preferential evaporation of $FeCl_2$, we calculate in Figure 5, gas phase energies for the loss of chlorine from $FeCl_3$, $FeCl_2$ and FeCl molecules. Results are reported based on PAW-GGA and M062X DFT methods. The latter is performed with the aid of Gaussian09 program.[27] Correponding results from previous CCSD theoretical predictions[28] are also presented for comparison. Values in Figure 5 supports the general energrtic trend that Fe-Cl bond in $FeCl_2$ molecule is significantly stronger than Fe-Cl bonds in $FeCl_3$ and FeCl molecules.[28] Thus, any desorbed $FeCl_2$ molecules are likely to be long-lived species while a relatively weaker bond in FeCl may results in its rapid dissotiation into Fe and Cl atoms. $FeCl_2$ could also form via addition of chlorine atoms to FeCl molecules.

Surface energies of Cl/Fe(100)

Figure 6 shows the surface free energies as a fuction of chlorine chemical potential. Pressure-temperture bar lins are presented for T=800, 900 and 1000 K for a very wide ranges of pressures. The choice of these particular temperatures stems from the fact that they simulate high-temperatures interactions of chlorine atoms with the Fe(100) surface in relevance to chlorination of organic pollutants.[29] Though, surface free energies could readily be established for any combination of temperatures and pressures based on E_{chem} values given in Tables 3 and 5. Figure 6 exhbit thermodynamic stability for all the above top, bridge,

hollow, mixed and substituational adsorption modes with different coverage. Schemitic strctures are given in Figures 1 and 2 with a brife describtion in Tables 3, 4 and 5. As shown in Figure 5, slopes of all stability lines increase with the chlorine coverage. Stability lines for S5 and S6 structures resides above the stability line of the S2 structure, and hence they are not shown in Figure 6.

In a very dillute chlorine environment ($\Delta\mu_{Cl} < -2.55$ eV), the clean Fe(100) surface is the thermodynamically most stable phase. Upon increasing the chlorine chemical potential over the narrow range of $-2.55 \text{ eV} < \Delta\mu_{Cl} < -2.35 \text{ eV}$, the H-1/9 confuguration becomes more stable that the clean surface. This chemical potential correponds to a pressure and temperature of T = 800 K for *P* (10^{-17} – 10^{-15}) atm., or *T* = 900 K for *P* (10^{-13} – 10^{-11}) atm,…etc. Over a short chlorine chemical potential range of $-2.35 \text{ eV} < \Delta\mu_{Cl} < -0.75 \text{ eV}$, the structures B-0.50 and H-0.50 become the favourable configurations with an almost degenerate thermodynamic stability. Increasing the chemical potential to values greater than -0.75 eV prefers the formation of the M-1.00 configuration.

Clearly, the stability trend depends strongly on the applied chemical potential. The variation of the most thermodynamic configuration from 1/9 to 1.00 is partially in line with experimental measurements that the maximum possible coverage of chlorine on Fe(100) surface amount to 0.74. However, it should be noted that formation of Cl/Fe(100) is most likely to be also governed by kinetic factors such as etching. All substituational adsorption structures (S1-S6) are thermodynamically less stable than their corresponding pure surface adsorption at a given coverage. In an analogy to the system of Cl/Cu(100), surface energetics for substituational adsorptions shows more variation than their corresponding pure surface structures at a given coverage.[9] This can be inferred by comparing stability lines for S1 and S2 with their corresponding pure surface adsorptions of B-0.25 and B-0.50; respectively. As discussed above, combining surface and sub-surface adsorptions results the formation of the S5 structure with coverage of 2.00 ML. The S5 structure resembles closely a $FeCl_2$(100) surface terminated with chlorine atoms. The very low thermodynamic stability of S5 indicates that formation of a $FeCl_2$ bulk is not feasible from a thermodynamic perspective.

Conclusions

Interaction between atomic chlorine and the Fe(100) surface is investigated using DFT cand ab initio atomitic thermodynamic calculations. Pure on-surface adsorptions are generally prefered over susbtitutational adsorptions. The highest possible coverage is found to amount to 0.50 ML. A *T-P* thermodynamic stability diagram is constructured by plotting caclulated surface free energies for Cl/Fe(100) configurations as a function of chlorine chemical potentials. It is predicted chlorine adsorption with a coverage of 0.50 ML at both hollow and brige sites provides the optimial adsorpative configurations at intermediate temperatures and a wide range of operating pressures. Increasing chlorine concentrations prefers full coverage , (i.e.; Θ = 1.00 ML) at mixed hollow and hollow sites. The ultimate objective is to create a Wulff construction diagarm that comprimises all chlorine – iron surfaces. This necesstaties adressing atomic chlorine adsorption on Fe(110) and Fe(111) surfaces as well.

Acknowledgment

The authors acknowledge access to the computational facilities of the Australian National Computational Infrastructure (NCI).

References

1 N. J. Welham, K. A. Malatt,S. Vukcevic, *Hydrometallurgy*, 2000, **57**, 209.
2 A. G. El Samrani, B. S. Lartiges, E. Montargès-Pelletier, V. Kazpard, O. Barrès,J. Ghanbaja, *Water. Res*, 2004, **38**, 756.
3 J. P. Lu, M. R. Albert, S. L. Bernasek,D. J. Dwyer, *Surf. Sci*, 1989, **215**, 348.
4 W.-H. Hung, J. Schwartz,S. L. Bernasek, *Surf Sci*, 1991, **248**, 332.
5 J. P. Lu, M. R. Albert,S. L. Bernasek, *Surf. Sci*, 1989, **217**, 55.
6 T. T. Suzuki, S. Entani,Y. Yamauchi, *Surf. Sci*, 2008, **602**, 1688.
7 S. Peljhan,A. Kokalj, *J. Phys. Chem. C*, 2009, **113**, 14363.

8 I. A. Suleiman, M. W. Radny, M. J. Gladys, P. V. Smith, J. C. Mackie, E. M. Kennedy,B. Z. Dlugogorski, *J. Phys.Chem. C*, 2011, **115**, 13412.
9 I. A. Suleiman, M. W. Radny, M. J. Gladys, P. V. Smith, J. C. Mackie, E. M. Kennedy,B. Z. Dlugogorski, *Phys. Chem. Chem.Phys*, 2011, **13**, 10306.
10 P. A. Dowben,R. G. Jones, *Surf. Sci*, 1979, **84**, 449.
11 S. Hino,R. M. Lambert, *Langmuir*, 1986, **2**, 147.
12 Š. Pick, *Surf. Sci*, 2008, **602**, 3733.
13 W. Zhao, J. Wang, F. Liu,D. Chen, *Chines. Sci. Bull*, 2009, **54**, 1295.
14 C. Stampfl, *Catalysis Today*, 2005, **105**, 17.
15 G. Kresse,J. Furthmüller, *Phys. Rev. B*, 1996, **54**, 11169.
16 P. E. Blöchl, *Phys. Rev. B*, 1994, **50**, 17953.
17 S. C. Jung,M. H. Kang, *Phys. Rev. B*, 2010, **81**, 115460.
18 W.-X. Li, C. Stampfl,M. Scheffler, *Phys. Rev. B*, 2003, **68**, 165412.
19 W. Zhong, G. Overney,D. Toma´nek, *Phys. Rev. B*, 1993, **47**, 95.
20 C. Kittel *Introduction in Solid State Physics*; Wiley: New York, 1986.
21 H. L. Zhang, S. Lu, M. P. J. Punkkinen, Q. M. Hu, B. Johansson,L. Vitos, *Phys. Rev. B*, 2010, **82**, 132409.
22 P. Błoński, A. Kiejna,J. Hafner, *Surf. Sci*, 2005, **590**, 88.
23 K. O. Legg, F. Jona, D. W. Jepsen,P. M. Marcus, *J. Phys. C*, 1977, **10**, 937.
24 M. Eder, K. Terakura,J. Hafner, *Phys. Rev.B*, 2001, **64**, 115426.
25 M. Alde´n, S. Mirbt, H. L. Skriver, N. M. Rosengaard,B. Johansson, *Phys. Rev. B*, 1992, **46**, 6303.
26 R. J. Sime,N. W. Gregory, *J. Phys. Chem*, 1960, **64**, 86.
27 M. J. T. Frisch, G. W.; Schlegel, H. B.; Scuseria, G. E.; Robb, M. A.; Cheeseman, J. R.; Scalmani, G.; Barone, V.; Mennucci, B.; Petersson, G. A.; Nakatsuji, H.; Caricato, M.; Li, X.; Hratchian, H. P.; Izmaylov, A. F.; Bloino, J.; Zheng, G.; Sonnenberg, J. L.; Hada, M.; Ehara, M.; Toyota, K.; Fukuda, R.; Hasegawa, J.; Ishida, M.; Nakajima, T.; Honda, Y.; Kitao, O.; Nakai, H.; Vreven, T.; Montgomery, Jr., J. A.; Peralta, J. E.; Ogliaro, F.; Bearpark, M.; Heyd, J. J.; Brothers, E.; Kudin, K. N.; Staroverov, V. N.; Kobayashi, R.; Normand, J.; Raghavachari, K.; Rendell, A.; Burant, J. C.; Iyengar, S. S.; Tomasi, J.; Cossi, M.; Rega, N.; Millam, J. M.; Klene, M.; Knox, J. E.; Cross, J. B.; Bakken, V.; Adamo, C.; Jaramillo, J.; Gomperts, R.; Stratmann, R. E.; Yazyev, O.; Austin, A. J.; Cammi, R.; Pomelli, C.; Ochterski, J. W.; Martin, R. L.; Morokuma, K.; Zakrzewski, V. G.; Voth, G. A.; Salvador, P.; Dannenberg, J. J.; Dapprich, S.; Daniels, A. D.; Farkas, Ö.; Foresman, J. B.; Ortiz, J. V.; Cioslowski, J.; Fox, D. J. ; A.1 ed.; Gaussian, Inc: Wallingford CT, 2009.
28 R. D. Bach, D. S. Shobe, H. B. Schlegel,C. J. Nagel, *J. Phys. Chem*, 1996, **100**, 8770.
29 M. Altarawneh, B. Z. Dlugogorski, E. M. Kennedy,J. C. Mackie, *Prog. Energy .Combust. Sci.*, 2009, **35**, 245.

Table 1. Calculated and lietrature properties for bulk bcc Fe.

	Calculated	Experimental [20]	Other calculated
Lattice constnat (Å)	2.828	2.845	2.830 [17]
Bulk-Modulus (GPa)	192	166 -173	169 - 201[21]
Magnetic moment (μ_B)	2.20	2.22	2.18, 2.21 [22]
Cohesive energy (eV)	-4.92	-4.28	-5.17[17]

Table 2. Calculated and lietrature properties for the Fe(100) surface.

Relaxation	Calculated	Experimental [23]	Other calculated
d_{12}(%)	-3.0	-1.4 ± 3.0	-3.50[24]
d_{23}(%)	1.7	5.0 ± 2.0	2.30[25]
Manetic moment for first layer (μ_B)	2.91		2.98 [25]
Manetic moment for second layer (μ_B)	2.34		2.35[25]

Table 3. Binding energies (E_b) and chemisrobed energies (E_{chem}) for perfect on-surface Cl/Fe(100) configurations. Values are in eV.

Θ	**Structure**	E_b	E_{chem}	**Θ**	**Structure**	E_b	E_{chem}
0.11	**B-1/9**	-3.97	-2.51	**0.11**	**T-1/9**	-2.78	-1.32
0.25	**B-0.25**	-3.93	-2.47	**0.25**	**T-0.25**	-2.72	-1.26
0.50	**B-0.50**	-4.02	-2.40	**0.50**	**T-0.50**	-3.71	-2.10
0.75	**B-.075**	-3.39	-1.73	**0.75**	**T-.075**	-3.29	-1.63
1.00	**B-1.00**	-3.09	-1.40	**1.00**	**T-1.00**	-2.74	-1.05
0.11	**H-1/9**	-4.02	-2.56	**0.50**	**M-0.50**	-3.55	-1.94
0.25	**H-0.25**	-3.87	-2.41	**0.75**	**M-0.75**	-3.53	-1.87
0.50	**H-0.50**	-3.99	-2.38	**1.00**	**M-1.00**	-3.28	-1.59
0.75	**H-0.75**	-3.50	-1.84				

Table 4. Summary of optimised geometries for perfect Cl/Fe(100) streuctures. All distances are in Å.

Θ	*d*(Cl-Fe)[a]	*Z*[b]	*h*[c]	d_{12}(%)[d]
B-1/9	2.330	2.049	0.165	1.094
B-0.25	2.336	1.978	0.166	2.540
B-0.50	2.331	1.878	0.013	4.680
B-.075	2.271	1.819	0.094	6.758
B-1.00	2.210	1.792	0.010	9.429
H-1/9	2.550	1.642	0.006	1.620
H-0.25	2.570	1.654	0.005	2.566
H-0.50	2.582	1.625	0.013	7.251
H-0.75	2.511	1.619	0.211	9.591
T-1/9	2.200	2.331	0.156	-1.280
T-0.25	2.174	2.276	0.232	-3.190
T-0.50	2.144	2.136	0.019	3.498
T-.075	2.154	2.161	0.065	6.671
T-1.00	2.148	2.151	0.073	7.391
M-0.50	2.425	1.822	0.019	7.915
M-0.75	2.460	1.709	0.014	7.582
M-1.00	2.410	1.624	0.013	9.906

[a]: Average of distance between Cl atom(s) and the nearest Fe atoms, [b]: average of heights of Cl atoms above the first layers, [c]: the height between the highest and lowest surface Fe atoms, [d]: relaxationof first and second Fe layers with respect to the clean optimised Fe(100) surface.

Table 5. Descriptions, coverages and chemisrobed energies (E_{chem}) for susbtituted Cl/Fe(100) configurations. Values are in eV.

Surface	Description	Θ	E_{chem}
S1	One first-layer Fe atom is substituted with a chlorine atom	**0.25**	**-2.16**
S2	Two first-layer Fe atoms are substituted with a chlorine atom	**0.50**	**-2.09**
S3	Three first-layer Fe atoms atom are substituted with a chlorine atom	**0.75**	**-1.30**
S4	All first-layer Fe atoms are substituted with a chlorine atom	**1.00**	**-1.23**
S5	All first- and second layers Fe atoms are substituted with a chlorine atom	**2.00**	**-0.07**
S6	One second-layer Fe atom is substituted with a chlorine atom	**0.25**	**-1.33**

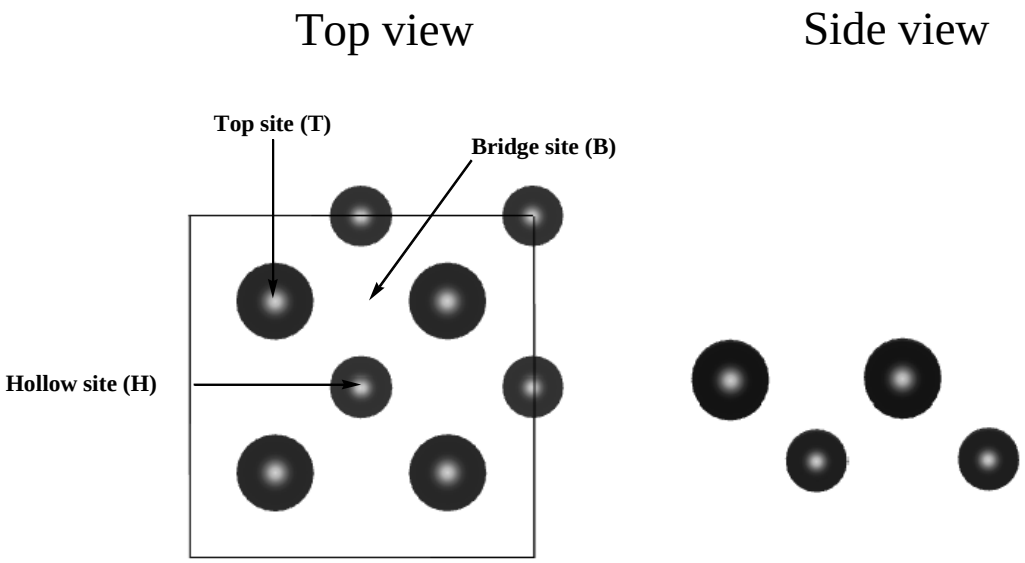

Figure 1: Top and side views of the first and second layer of the Fe(100) surface. Larger and small spheres denote first-layer and second-layer Fe atoms; respectively.

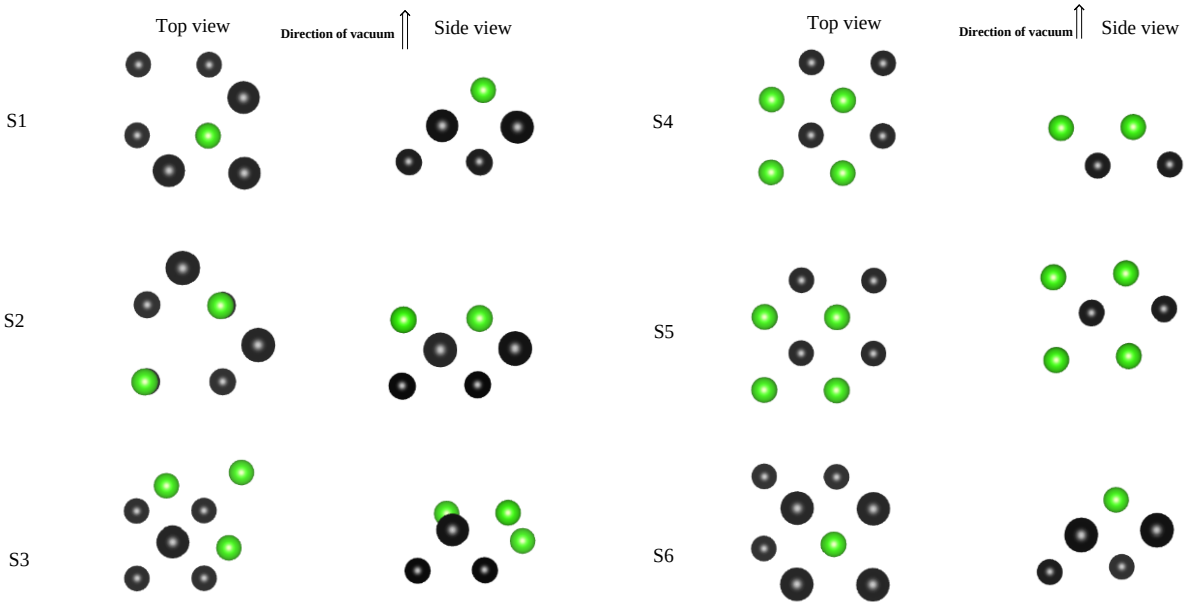

Figure 2: Top and side views susbtituted Cl/Fe(100) configurations. Larger dark and small dark spheres denote first-layer and second-layer Fe atoms; respectively.

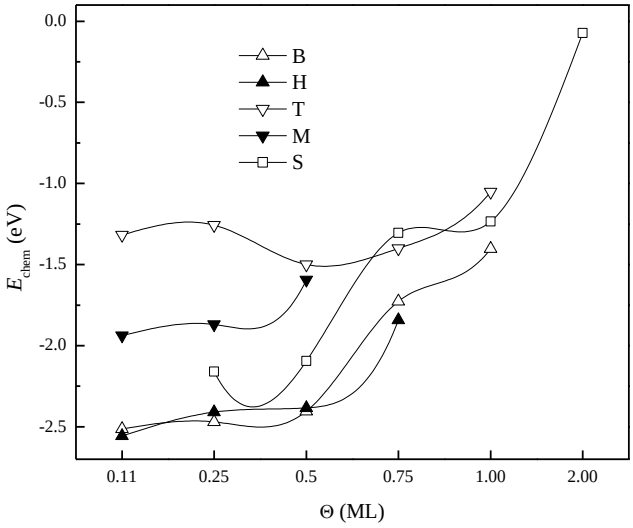

Figure 3: Trend of chemisrobed energies (E_{chem}) with the coverage.

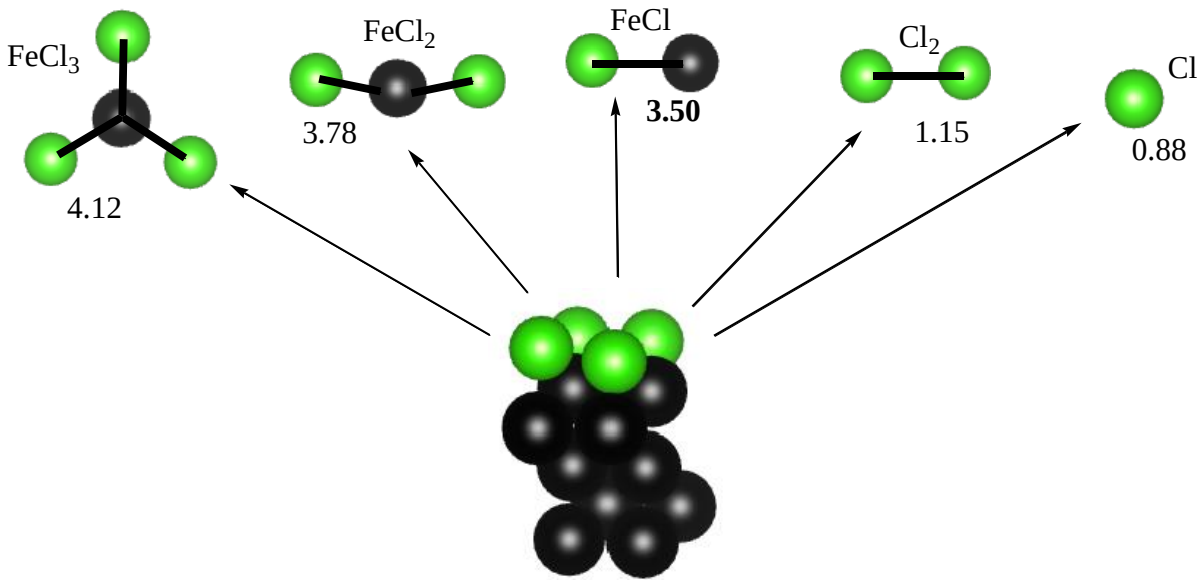

Figure 4: Calculated sublimation energies for the evaporation of $FeCl_3$, $FeCl_2$, FeCl, Cl_2 and Cl from the M-1.00 structure. Dark spheres denote Fe atoms. Values are in eV.

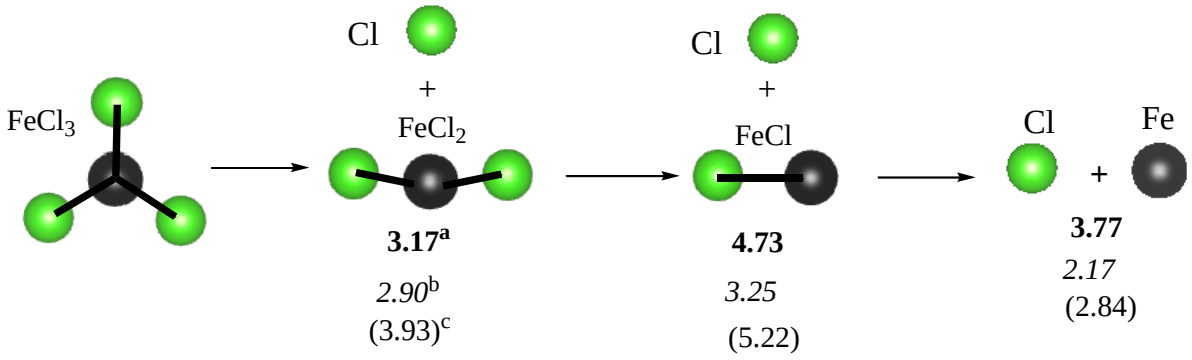

Figure 5: Calculated gas phase Fe-Cl bond dissociation energies in $FeCl_3$, $FeCl_2$, FeCl. Dark spheres denote Fe atoms. Values in bold, italic and in brackets referee to PAW-GGA, M062X and CCSD [28] calculations; respectively. All values are in eV.

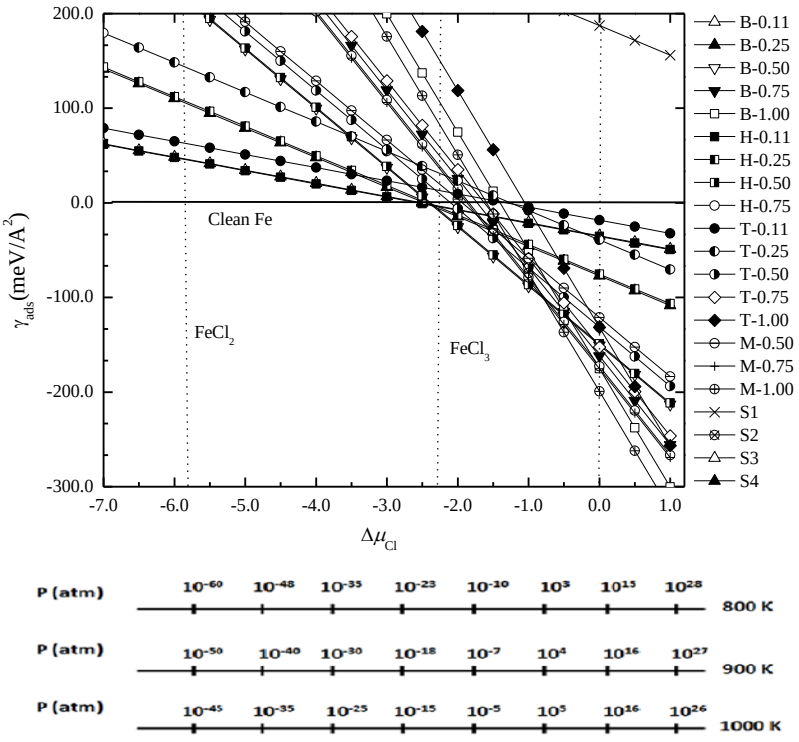

Figure 6: Surface free energy for Cl/Fe(100) structures as a function of the chlorine chemical potential.